European Journal of Medicinal Chemistry 49 (2012) 151–163

Contents lists available at SciVerse ScienceDirect

European Journal of Medicinal Chemistry

journal homepage: http://www.elsevier.com/locate/ejmech

Original article

Novel metal based anti-tuberculosis agent: Synthesis, characterization, catalytic and pharmacological activities of copper complexes

J. Joseph*, K. Nagashri, G. Boomadevi Janaki

Department of Chemistry, Noorul Islam Centre for Higher Education, Kumaracoil 629 180, Tamilnadu, India

ARTICLE INFO

Article history:
Received 19 August 2011
Received in revised form
16 November 2011
Accepted 5 January 2012
Available online 18 January 2012

Keywords:
Screening
Antioxidant
Inhibition
Superoxide dismutase
Cleavage
Copper

ABSTRACT

Copper complexes of molecular formulae, $[CuL^1(OAc)]$, $[CuL^2(H_2O)]$, $[CuL^3(H_2O)]$, $[CuL^4(H_2O)]$, $[CuL^5(H_2O)]$ where L^1–L^5 represents Schiff base ligands [by the condensation of 3-hydroxyflavone with 4-aminoantipyrine (L^1)/*o*-aminophenol (L^2)/*o*-aminobenzoic acid (L^3)/*o*-aminothiazole (L^4)/thiosemicarbazide (L^5)], have been prepared. They were characterized using analytical and spectral techniques. The DNA binding properties of copper complexes were studied using electronic absorption spectra and viscosity measurements. Superoxide dismutase and antioxidant activities of the copper complexes have also been studied. Furthermore, the copper complexes have been found to promote pUC18 DNA cleavage in the presence of oxidant. Anti-tuberculosis activity was also performed.

1. Introduction

Several classes of antimicrobial compounds are presently available; microorganism's resistance to these drugs constantly emerges. In order to prevent this serious medical problem, the elaboration of new types of antibacterial agents or the expansion of bioactivity of the naturally known biosensitive compounds is a very interesting research problem. The synthesis and characterization of metal complexes with organic bioactive ligands is one of the promising fields for the search, in particular, of copper complexes with derivatives of hydroxyflavone.

Deoxyribonucleic acid (DNA) is the primary target molecule for most anticancer and antiviral therapies according to cell biologist. Investigations on the interaction of DNA with small molecules are important in designing new types of pharmaceutical molecules. The important criteria for the development of metallodrugs as chemotherapeutic agents are the ability of the metallo drug to bring about DNA cleavage. A large number of transition metal complexes have been found to promote DNA cleavage because of their redox properties. Transition metal complexes have been reported to bring about DNA cleavage either oxidatively or hydrolytically or photolytically.

Metal complexes of Schiff base ligands have been investigated as models for active sites of enzymes [1,2], including DNA cleavage systems [3,4], and as antibacterial [5–7] and anticancer [8] drugs. Metal complexes of S-, N-, and O-chelating ligands have attracted the considerable attention because of their interesting physico–chemical properties, pronounced biological activities, and as models of metalloenzyme active sites [9,10]. Schiff bases and their transition metal complexes have been used as anticancer, antituberculer, antibacterial, antifungal, hypertensive and hypothermic reagents [11–13].

Copper has a wide spectrum of effectiveness against a variety of microorganisms and thus copper-containing compounds such as Bordeaux mixture, copper sulphate, etc., have been used for the control of plant pathogenic fungi and bacteria on most agricultural crops [14]. Natural chelating agents can reduce copper toxicity by binding part of the available copper and protect against the toxicity of copper towards bacteria and fungi [15]. As transition metal ions play a vital role in the initiation of free radical processes (*via* the Fenton reaction), metal chelation is widely considered as another mechanism of the antioxidant activity of flavonoids. The interaction of metal ions with flavonoids may change the antioxidant properties and some biological effects of the flavonoids [16].

The structural modifications of promising lead compounds are still a major line of approach to develop new therapeutic agents. It involves an intensive effort to condense the different pharmacophoric groups of bioactive active moieties into one compound, and

* Corresponding author. Tel.: +91 4651 366295, +91 9629474150.
E-mail address: chem_joseph@yahoo.co.in (J. Joseph).

0223-5234/$ – see front matter © 2012 Elsevier Masson SAS. All rights reserved.
doi:10.1016/j.ejmech.2012.01.006

it may behave as chemotherapeutic agents. Due to the diversified nature, hydroxyflavone derivatives is a useful substance in medicinal research. In the present study, we report the synthesis and biochemical activities of copper complexes with hydroxyflavone derivatives.

2. Chemistry

Ligands were synthesized by the reaction of 3-hydroxyflavone and 4-aminoantipyrine/o-aminophenol/o-aminobenzoicacid/o-aminothiazole/thiosemicarbazide (targeted compounds are shown in Scheme 1). The complexes were obtained by refluxing the equimolar solutions of copper acetate and ligand (s). The copper complexes were obtained as solids in different yields. The purity of synthesized compounds was confirmed by TLC and elemental analysis. C, N and H analysis were carried out micro analytically. Magnetic moments were determined at room temperature. They are insoluble in acetone, ethanol, benzene and chloroform, but their considerable solubility has been noticed in DMF and DMSO. The complexes are stable at room temperature. They are non-hygroscopic and can be stored for a long length of period without decomposition. The structures of the synthesized compounds were confirmed by analytical and spectral data (IR, ^{1}H & ^{13}C NMR, ESR and FAB mass).

3. Pharmacology

The *in vitro* evaluation of antimicrobial activity was carried out. The purpose of the screening program is to provide antimicrobial efficiencies of the investigated compounds. The prepared compounds were tested against some fungi and bacteria to provide the minimum inhibitory concentration (MIC) for each compound. MIC is the lowest concentration of solution to inhibit the growth of a test organism. The *in vitro* antimicrobial activities of the investigated compounds were tested against the bacterial species,

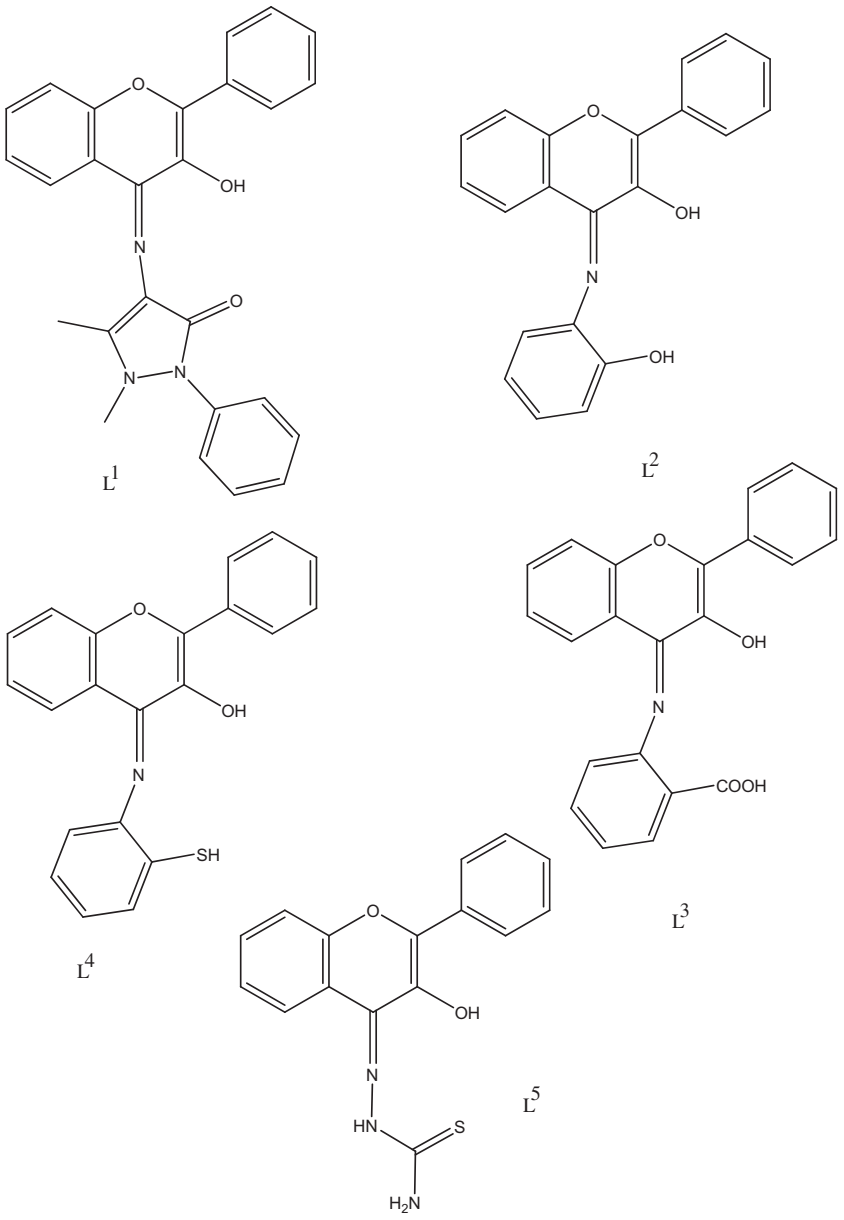

Scheme 1. Targeted compounds (L^1–L^5).

Table 1
Electronic spectral data of ligands and their copper complexes.

S.No	Compound	Solvent	Absorption (nm)	Band assignment	Geometry
1	L^1	DMSO	268	INCT	–
2	L^2	DMSO	282	INCT	–
			498	INCT	
3	L^3	DMSO	248	INCT	–
			342	INCT	
4	L^4	DMSO	234	INCT	–
			342	INCT	
5	L^5	DMSO	246	INCT	–
			358	INCT	
6	$[CuL^1(OAc)]$	DMSO	251	INCT	Square planar
			342	INCT	
			578	$^2B_{1g} \rightarrow {}^2A_{1g}$	
7	$[CuL^2(H_2O)]$	DMSO	248	INCT	Square planar
			352	INCT	
			530	$^2B_{1g} \rightarrow {}^2A_{1g}$	
8	$[CuL^3(H_2O)]$	DMSO	254	INCT	Square planar
			348	INCT	
			572	$^2B_{1g} \rightarrow {}^2A_{1g}$	
9	$[CuL^4(H_2O)]$	DMSO	241	INCT	Square planar
			348	INCT	
			544	$^2B_{1g} \rightarrow {}^2A_{1g}$	
10	$[CuL^5(H_2O)]$	DMSO	260	INCT	Square planar
			351	INCT	
			538	$^2B_{1g} \rightarrow {}^2A_{1g}$	

Staphylococcus aureus, *Escherichia coli*, *Klebsiella pneumoniae*, *Proteus vulgaris* and *Pseudomonas aeruginosa* and fungal species, *Aspergillus niger*, *Rhizopus stolonifer*, *Aspergillus flavus*, *Rhizoctonia bataicola* and *Candida albicans*. The Superoxide dismutase and antioxidant activities of copper complexes were measured [17]. The DNA binding and cleavage studies of copper complexes were also studied. Anti-tuberculosis activity was also performed. In addition, catalytic activity of copper complexes was also performed by the conversion of benzene into phenol in the presence of hydrogen peroxide.

4. Results

The UV–Vis., and ESR spectral data of ligands and their copper complexes are recorded in DMSO and are presented in Tables 1 and 2. The redox behaviour of copper complexes were measured in DMSO and summarized in Table 3. In addition, the inhibitory values obtained for compounds against bacteria and fungi and are tabulated in Tables 4 and 5. The superoxide dismutase (SOD) mimetic activity (IC_{50}) of the synthesized complexes are summarized in Table 6. The binding constant for copper complexes with CT DNA are presented in Table 7. Furthermore, *in vitro* anti-tubercular screening data of synthesized compounds are summarized in Table 8.

Table 3
Cyclic voltammetric data of copper complexes.

Complex	E_{pa}	E_{pc}	ΔE_p	Potential assignment
$[CuL^1(OAc)]$	−0.258	−0.166	118	Cu(II)/Cu(I)
$[CuL^2(H_2O)]$	−0.592	−0.748	158	Cu(II)/Cu(I)
	1.16	–		Ligand oxidation
$[CuL^3(H_2O)]$	−0.632	−0.772	140	Cu(II)/Cu(I)
	0.465	–	–	Cu(II)/Cu(III)
$[CuL^4(H_2O)]$	−0.606	−0.778	169	Cu(II)/Cu(I)
	0.436	−0.597	–	Cu(I)/Cu(0)
$[CuL^5(H_2O)]$	−0.655	−0.768	116	Cu(II)/Cu(I)
	0.424	−0.568		Cu(I)/Cu(0)

5. Discussion

The elemental analysis and mass spectrum were good agreement with the formation of 1:1 (metal:ligand) stoichiometry. All complexes were decomposed above 280 °C indicating their thermal stability. The molar conductance data for the copper complexes were measured in DMSO solution are given in experimental section. The values of complexes fall in the range of 8–29 Ω^{-1} cm^2 mol^{-1}, which is the expected range of 1–35 Ω^{-1} cm^2 mol^{-1} for the complexes to behave as non-electrolytes [18,19]. Thus, the complexes have non-electrolytic nature as evidenced by the involvement of acetate group in coordination.

Mass spectra provide a vital clue for elucidating the structure of compounds. The mass spectra of the ligand (L^1) and its copper complex $[CuL^1(OAc)]$ were recorded and their stoichiometric compositions were compared. The intensity of these peaks reflects the stability and abundance of the ions [20]. The molecular ion peak for the ligand (L^1) is observed at424 *m/z* whereas its copper complex shows the molecular ion peak at 515 *m/z*, which confirms the stoichiometry of the metal complexes to be $[CuL^1(OAc)]$ type. Elemental analysis values are in close agreement with the values calculated from molecular formula assigned to these complexes, which is further supported by the FAB-mass studies of respective complexes. Similar mass spectral features were assigned for other ligands and their copper complexes. The different pathways of the fragments of the parent molecular ion peaks are given in Scheme 2. The stoichiometry is confirmed by the mass spectra of complexes.

The IR spectrum of the ligands show a ν(C=N) peak in the region 1645-1632 cm^{-1}. The IR spectra of all complexes show ν(C=N) bands shifted to lower frequency of at 1629–1590 cm^{-1} [20] which indicates that the azomethine nitrogen is one of the coordinating atoms in the Schiff bases. However, the spectra of complexes show two characteristic bands at 1630–1602 and 1404–1344 cm^{-1} attributed to $\upsilon_{asy}(COO^-)$ and $\upsilon_{sy}(COO^-)$ respectively, indicating the participation of the carboxylate oxygen atom in the complexes. The mode of coordination of carboxylate group has often been

Table 2
ESR spectral data of the copper complexes.

Complex	$g_{\|\|}$	$g\perp$	g_{iso}	$A_{\|\|}$	$A\perp$	$K_{\|\|}$	$K\perp$	α^2	β^2	γ^2	$f(g_{\|\|}/A_{\|\|})$
$[CuL^1(OAc)]$ at 300 K			2.08								
$[CuL^1(OAc)]$ at 77 K	2.24	2.05	–	150	42	0.91	0.56	0.74	1.3	0.75	150
$[CuL^2(H_2O)]$ at 300 K			2.12								
$[CuL^2(H_2O)]$ at 77 K	2.24	2.06	–	146	38	0.85	0.42	0.78	1.5	0.72	153
$[CuL^3(H_2O)]$ at 300 K			2.06								
$[CuL^3(H_2O)]$ at 77 K	2.22	2.05	–	154	50	0.78	0.52	0.83	1.4	0.81	144
$[CuL^4(H_2O)]$ at 300 K			2.10								
$[CuL^4(H_2O)]$ at 77 K	2.20	2.05	–	156	52	0.76	0.51	0.83	1.2	0.80	141
$[CuL^5(H_2O)]$ at 300 K			2.08								
$[CuL^5(H_2O)]$ at 77 K	2.21	2.05	–	154	54	0.75	0.51	0.80	1.4	0.82	143

Table 4
Minimum inhibitory of concentration of the synthesized compounds against growth of bacteria (μM).

S.No	Compound	*E. coli*	*K. pneumoniae*	*S. typhi*	*P. aeruginosa*	*S. aureus*
1	L^1	60	64	66	66	72
2	L^2	24	26	20	16	28
3.	L^3	28	36	26	32	30
4	L^4	60	64	66	66	72
5	L^5	24	26	20	16	28
6	$[CuL^1(OAc)]$	34	38	32	28	42
7	$[CuL^2(H_2O)]$	26	28	30	26	48
8	$[CuL^3(H_2O)]$	52	54	58	60	63
9	$[CuL^4(H_2O)]$	34	38	32	28	42
10	$[CuL^5(H_2O)]$	26	28	30	26	48
11	Ampicillin	12	10	08	04	06
12	Vancomycin	06	14	12	10	08
13	Ofloxacin	08	10	04	06	14

deduced from the magnitude of the observed separation between the $\upsilon_{asy}(COO^-)$ and $\upsilon_{sy}(COO^-)$, the separation value (A) between $\upsilon_{asy}(COO^-)$ and $\upsilon_{sy}(COO^-)$ in metal complexes was more than 200 cm^{-1} (260–216 cm^{-1}) suggests the coordination of carboxylate group in copper complexes of the ligands in a monodentate fashion [21]. The Schiff base ligand (L^4) displays band around 844 cm^{-1} ascribed to υ C–S–C [21] which shifts to lower frequencies in their spectra of copper complexes in the region 838–832 cm^{-1}, respectively, suggesting the coordination of copper ions through the sulphur atom of thioazole moiety. The band at 3466 cm^{-1} for υ(OH) in the free ligand disappeared on complexation, indicating coordination through a deprotonated oxygen. In the IR spectra of the ligand (L^5), two sharp bands at ca. 3436 and 3352 cm^{-1}, probably due to asymmetric and symmetric vibrations of the NH_2 group, do not undergo any change in the spectra of the complexes indicating the non-involvement of the NH_2 group on coordination. In the spectrum of copper complexes, the coordination of azomethine nitrogen atom is further substantiated by the observed positive shift of 34–48 cm^{-1} in the N–N stretching mode in the complexes. Monodentate coordination of the N–N moiety is reported to increase its stretching frequency by this amount. The absence of thioamide band ν(HN–C=S) at *ca* 782–813 cm^{-1} and the appearance of new band at ca. 610–631 cm^{-1} confirmed the conversion of ν(C=S) into ν(C–S) band. The reduction of thioamide band ν(N=C–SH) observed at ca 982 cm^{-1} suggests that coordination occurs through S atom. The IR spectra of complexes show new band due to the stretching vibrations of >C=N–N=C< bonds at 1568–1560 cm^{-1}. The band observed in the region 1534–1526 cm^{-1} is due to the $\nu_{C=C}$ stretching of the aromatic ring system. In all the copper–Schiff base complexes, most of the band shifts observed in the wave number region 1142–980 cm^{-1} are in agreement with the structural changes observed in the molecular carbon skeleton after complexation, which cause some changes in (C–C) bond lengths. Conclusive evidence of the bonding is also shown by the observation that new bands in the spectra of all copper complexes appear in the low frequency regions at 550–516, 504–498 and 486–448 cm^{-1} characteristic to υ(M–O), υ(M–N) and υ(M–S) stretching vibrations, respectively, that are not observed in the spectra of both free ligands [22]. The IR bands at 810–854 and 784–799 cm^{-1}, $\upsilon(H_2O)$ of coordinated water, is an indication of the binding of the water molecules to the metal ions. Another band located at 522 cm^{-1} in the spectrum of [Cu(L)(OAc)] complex may be due to υ(M–O) of the acetate group. The IR spectrum of the ligand (L^5) and its copper complex are shown in figs (Supplementary material).

Table 5
Minimum inhibition of concentration of the synthesized compounds against growth of fungi (μM).

S.No	Compound	*A. niger*	*R. stolonifer*	*A. flavus*	*R. bataicola*	*C. albicans*
1	L^1	60	66	72	80	50
2	L^2	72	84	63	77	65
3	L^3	85	76	69	64	102
4	L^4	69	79	88	82	86
5	L^5	88	90	96	70	78
6	$[CuL^1(OAc)]$	28	30	34	38	32
7	$[CuL^2(H_2O)]$	32	26	46	36	38
8	$[CuL^3(H_2O)]$	52	55	68	80	50
9	$[CuL^4(H_2O)]$	28	30	34	38	32
10	$[CuL^5(H_2O)]$	32	26	46	36	38
11	Nystatin	10	16	8	14	12
12	Bavstatin	14	10	08	06	12

Table 6
Superoxide dismutase activity of some copper(II) complexes.

S.No	Complex	IC_{50} (μM)
1	$[CuL^1(OAc)]$	0.72
2	$[CuL^2(H_2O)]$	0.67
3	$[CuL^3(H_2O)]$	0.56
4	$[CuL^4(H_2O)]$	0.66
5	$[CuL^5(H_2O)]$	0.08
6	Native SOD	0.04

The electronic absorption spectra of the Schiff base ligands and their copper complexes in DMSO were recorded at room temperature and the band positions of the absorption maxima; band assignments and the proposed geometry are shown in experimental section. The electronic spectra of the ligands and their complexes were recorded in DMSO as a solvent. The absorption spectrum for L^1 shows band at 268 nm (Fig, Supplementary material). These bands can be attributed to n-π^* transitions within the Schiff base molecule. The electronic spectrum of the corresponding $[CuL^1(OAc)]$ complex in DMSO (Fig, Supplementary material) reveals a broad band at 498 nm assignable to $^2B_{1g} \rightarrow {}^2A_{1g}$ transition [23] which is characteristic of square planar environment around the copper(II) ion. Similar spectral features were assigned for other complexes and are tabulated (Table 1).

5.1. Stability of the complexes in solution

The stability of these targeted complexes in aqueous solution has been studied by observing the UV–Vis spectra and estimating the molar conductivities at different time intervals for any possible change [24]. The tested compounds were prepared in DMSO and for experiments freshly diluted in phosphate buffer system. Then, the UV–Vis., spectra and molar conductivities were measured at different time intervals. It can seen form the results show that there are no change absorption bands and their molar conductance values for freshly prepared solutions. It indicates these three complexes are quite stable in phosphate buffer.

Table 7
Absorption spectral properties of copper complexes.

Complex	λ_{max}	Free bound	$\Delta\lambda$ (nm)	K_b (M^{-1})
$[CuL^1(OAc)]$	386	380	6	1.4×10^6
$[CuL^2(H_2O)]$	368	360	8	2.1×10^6
$[CuL^3(H_2O)]$	388	381	7	1.9×10^6
$[CuL^4(H_2O)]$	385	378	7	2.4×10^5
$[CuL^5(H_2O)]$	376	371	5	3.0×10^5

Table 8
In vitro anti-tubercular screening data of synthesized compounds.

S.No	Compound	MIC ($\mu M \times 10^{-3}$)
1	L^1	44
2	L^2	40
3	L^3	52
4	L^4	60
5	L^5	34
6	$[CuL^1(OAc)]$	18
7	$[CuL^2(H_2O)]$	24
8	$[CuL^3(H_2O)]$	12
9	$[CuL^4(H_2O)]$	4
10	$[CuL^5(H_2O)]$	10
11	INH	2
12	CFL	9

The NMR spectra of the synthesized compounds give information about the skeleton of the compounds. The ^1H and ^{13}C NMR spectrum of ligands were recorded in $CDCl_3$ and are given in experimental section.

The ^1H NMR spectrum of the ligand (L^1) shows different signals and are assigned as follows: 6.6–7.5 ppm (14H, m, Ar–H), 1.6 ppm(3H, s, H_3C–C), 1.9 ppm(s, 3H, H_3C–N) and the peak at 10.8 ppm(1H, s, O–H, D_2O exchangeable) is attributable to the –OH group present in the 3-hydroxyflavone moiety, respectively. The ^{13}C NMR ligand (L^1) shows different signals and are assigned as follows: 12.5 ppm (H_3**C**–C), 19.6 ppm (H_3**C**–N), 143.5 ppm (H_3C–**C**), 162.8 ppm (**C**=O), 154.5 ppm (=C–N), 124.6 ppm (C-2), 118.8 ppm (C-3), 152.6 ppm (C-4), 119.2 ppm (C-5), 146.4 ppm (C-6), 125.2 ppm (C-7), 126.4 ppm (C-8), 157.3 ppm (C-9), 121.6 ppm (C-10), 133.8 ppm (C-1′), 127.4 ppm (C-2′, 6′), 141.8 ppm (C-3′, 5′), 133.5 ppm (C-4′), 127.2 ppm (C-1″), 119.6 ppm (C-2″, 6″), 118.9 ppm (C-3″, 5″) and 121.6 ppm (C-4″), respectively. All the protons

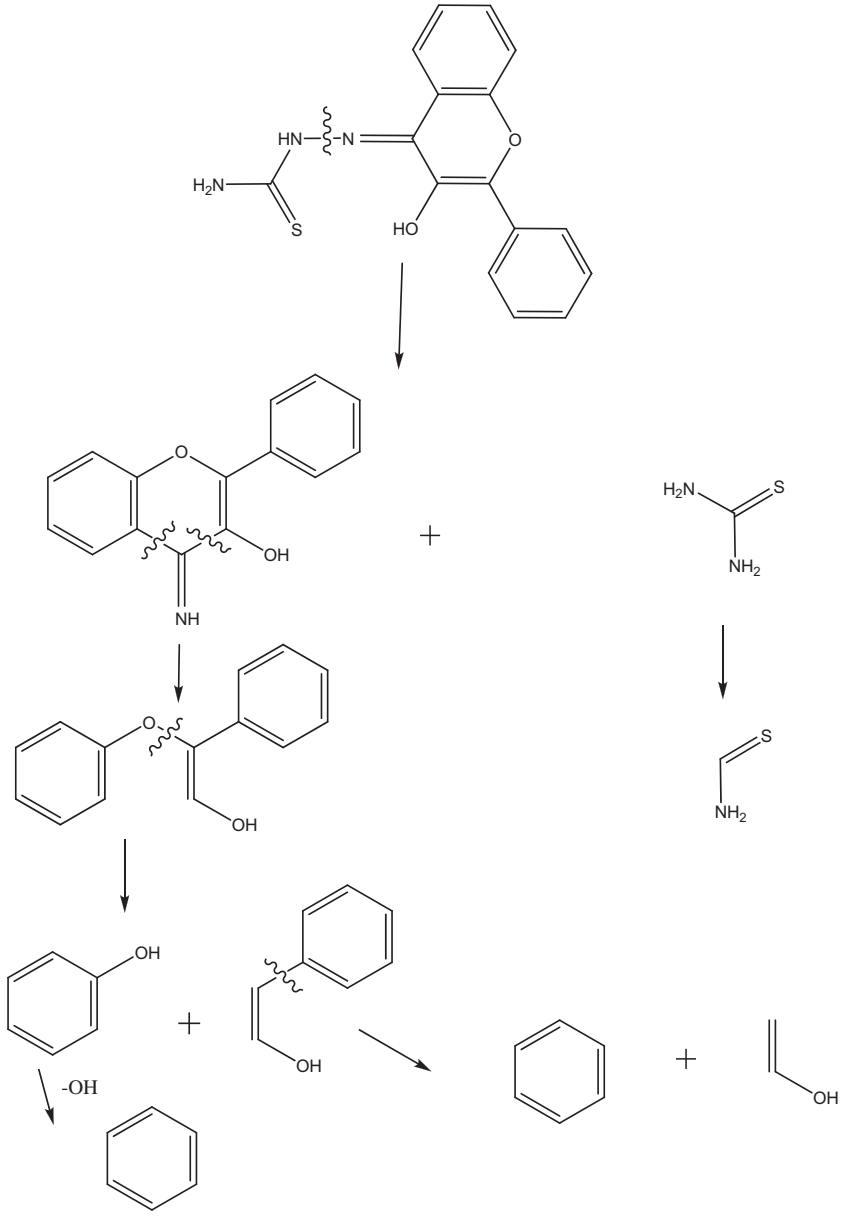

Scheme 2. Mass fragment pattern of L^5.

were found as to be in their expected region [25]. The number of protons calculated from the integration curves and those obtained from the values of the expected CHN analyses agree with each other.

The ESR spectrum of the [CuL^1(OAc)] complex was recorded in DMSO at 300 and 77 K. The spectrum at 300 K shows one intense absorption band at high field, which is isotropic due to the tumbling motion of the molecules. However, this complex in the frozen state shows four well resolved peaks with low intensities in the low field region and one intense peak in the high field region. The magnetic susceptibility value reveals that the copper complex has a magnetic moment of 1.94 B.M. corresponding to one unpaired electron, indicating that the complex is mononuclear in nature. This fact was also evident from the absence of half field signal, observed in the spectrum at 1600G due to the $m_s = \pm 2$ transitions, ruling out any Cu–Cu interaction [26] and confirms that the synthesized copper complexes are monomeric in nature [27]. The ESR spectral data are given in Table 2.

The value of $g_{||} < 2.3$ in the present complex gives a clear indication of covalent character of the metal–ligand bond and delocalisation of the unpaired electron into the ligand. The trend of $g_{||}(2.24) > g\perp(2.05) > g_e(2.0036)$ describes the axial symmetry with the unpaired electron residing in the $d_{x^2-y^2}$ orbital. For the present Cu(II) complex, the observed g values are $g||(2.24) > g\perp(2.05) > g_e(2.0036)$, which suggest that the unpaired electron lies in the $d_{x^2-y^2}$ orbital. The $A_{||}$ and $A_\perp$ values in the order: $A_{||}(150) > A_\perp(42)$ also indicate that the complex has square planar geometry and the system is axially symmetric [28]. In the present study, the f values for copper complexes were observed in the range of 141–153 cm^{-1}. It is suggested that the synthesized copper complexes exhibiting appreciable square planar distortion is expected to show high SOD like activity.

Molecular orbital coefficients α^2(in-plane σ-bonding), β^2(in-plane π-bonding) and γ^2(out-plane π-bonding) were calculated using Eqs. (1)–(3).

$$\alpha^2 = -\left(A_{||}/0.036\right) + \left(g_{||} - 2.0036\right) + 3/7(g_\perp - 2.0036) + 0.04 \quad (1)$$

$$\beta^2 = \left(g_{||} - 2.0036\right)E/ - 8\lambda\alpha^2 \quad (2)$$

$$\gamma^2 = (g_\perp - 2.0036)E/ - 2\lambda\alpha^2 \quad (3)$$

The α^2 value of 0.5 indicates complete covalent bonding, while that of 1.0 suggests complete ionic bonding. The observed value of 0.74 for the present complex indicates that the copper complex has some covalent character. The observed β^2 and γ^2 values of 1.3 and 0.75 indicate that there is interaction in the out-of-plane π-bonding, whereas the in-plane π-bonding is predominantly ionic. Significant information about the nature of bonding in the Cu(II) complex can be derived from the relative magnitudes of $K_{||}$ and $K\perp$.

$$K_{||} = \alpha^2\beta^2 \quad (4)$$

$$K_\perp = \alpha^2\gamma^2 \quad (5)$$

For the present complex, the observed order: $K_{||}(0.91) > K\perp(0.56)$ implies a greater contribution from out-of plane π-bonding than from in in-plane π-bonding in metal–ligand π bonding.

The electrochemical behaviours of the Schiff base Cu(II) complexes in DMSO (0.1 M of TBAP as supporting electrolyte (scan rate 100 mV s^{-1})) at 300 K were examined. The electrochemical data of copper complexes are given in Table 3. The cyclic voltammogram of the [CuL^1(OAc)] complex in DMSO solution at 300 K in the potential range +0.4 to −0.8 V at scan rate 0.1 Vs^{-1} was recorded (Fig. 1). It shows a well defined redox process corresponding to the formation of the quasi-reversible Cu(II)/Cu(I) couple. The anodic peak at Epa = −0.258 mV versus Ag/AgCl and the associated cathodic peak atEpc = −0.166 mV correspond to the Cu(II)/Cu(I) couple. The [CuL^1(OAc)] complex exhibits a quasi-reversible behaviour.

On comparing the cyclic voltammograms, we observed that the variation in oxidation and reduction potential may be due to distortion in the geometry of the complexes which arises due to different donor atoms coordinated to the copper ion. It is concluded that the present ligand systems stabilize the unusual oxidation states of copper ion during electrolysis. It is essential factor for pharmacological activities and plays a crucial role in curing or prevention of untreatable diseases. Similar electrochemical behaviour was observed and assigned for other complexes.

5.2. Thermal analysis

The thermogravimetric analyses for the copper complexes were carried out within a temperature range from 200 to 650 °C in N_2 atmosphere at a rate of 10 °C per minute in order to establish their compositional differences as well as to ascertain the nature of associated water molecules [29]. Water molecules were lost in between 50 and 300 °C and metal oxides were formed above 550 °C for all complexes. The copper chelates degrade into two stages. The first step corresponds to the loss of coordinated water molecule and acetate ion, respectively. The second step corresponds to the loss of ligand molecule that leads to the formation of copper oxide as a final product from which the percentage of copper content was calculated and compared with those obtained from AAS. The degradation pathway for all complexes may be represented as follows:

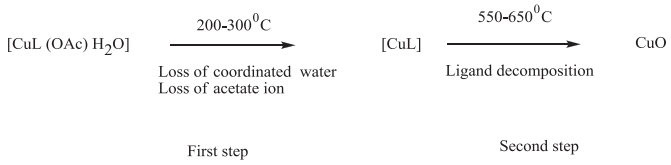

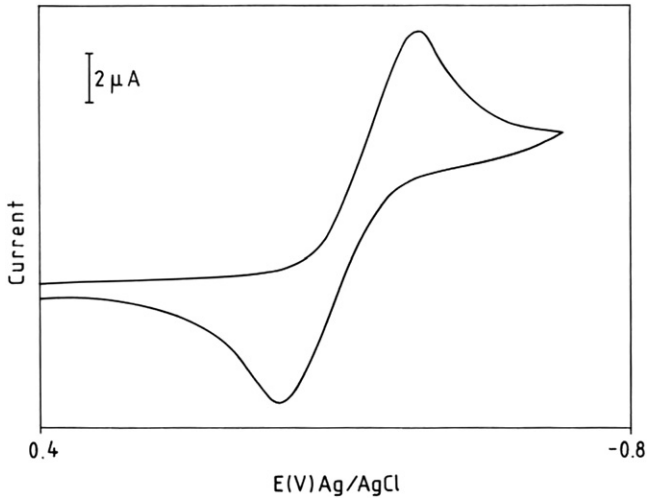

Fig. 1. Cyclic voltammogram of [CuL^1(OAc)] complex.

5.3. Powder XRD

The crystallite size of the complex was calculated from Scherre's formula:

$$d_{XRD} = 0.9\lambda/\beta\ \theta$$

where λ is the wavelength, β is the full-width half maximum of the characteristic peak and θ is the diffraction angle for the hkl plane.

From the observed d_{xRD} patterns, the average crystallite sizes for the $[Cu(L^1)(OAc)]$, $[CuL^2(H_2O)]$, $[CuL^3(H_2O)]$, $[CuL^4(H_2O)]$, $[CuL^5(H_2O)]$ complexes are found to be 75, 84, 92, 64 and 52 nm, respectively. The smaller grain sizes were found from XRD suggesting that these complexes are polycrystalline with nanosized grains.

5.4. SEM

The surface morphology of the copper complexes exhibited different morphology. The particle sizes of the Cu(II) complexes were in the diameter range of few microns. However, particles with sizes less than 100 nm were also observed which groups to form agglomerates of larger size. Such facts are in good agreement with the obtained powder XRD results.

5.5. Antimicrobial activity

The *in vitro* antimicrobial activities of the investigated compounds were tested against the bacterial species *S. aureus*, *E. coli*, *K. pneumaniae*, *P. vulgaris* and *P. aeruginosa* and fungal species *A. niger*, *R. stolonifer*, *A. flavus*, *R. bataicola* and *C. albicans*. The MIC values of the compounds are summarized in Tables 4 and 5. A comparative study of the ligands and their complexes indicates that complexes exhibit higher antimicrobial activity than the free ligands. In this study, the antimicrobial activity of the ligands may be due to the heteroaromatic residues. Compounds containing >C=N group have enhanced antimicrobial activity than >C=C< group. The growth of certain microorganisms takes place even in the absence of O_2. Hence, compounds containing >C=C< group though capable of absorbing O_2 are not related with the growth of microorganisms.

The enhanced activity of the complexes can be explained on the basis of Overtone's concept [30] and Tweedys Chelation theory [31]. According to Overtone's concept of cell permeability, the lipid membrane that surrounds the cell favours the passage of only the lipid-soluble materials which makes liposolubility an important factor which controls the antimicrobial activity. On chelation, the polarity of the metal ion will be reduced to a greater extent due to the overlap of the ligand orbital and partial sharing of the positive charge of the metal ion with donor groups. Further, it increases the delocalisation of π-electrons over the whole chelate ring and enhances the lipophilicity of the complexes. This increased lipophilicity enhances the permeation of the complexes into lipid membranes and blocking of the metal binding sites in the enzymes of microorganisms. These complexes also disturb the respiration process of the cell and thus block the synthesis of the proteins that restricts further growth of the organism and as a result microorganisms die.

The increased activity of the complexes can also be explained on the basis of their high solubility, fitness of the particles, size of the metal ion and the presence of the bulkier organic moieties. Another mechanism of toxicity of these complexes to microorganisms may be due to the inhibition of energy production or ATP production, by inhibiting respiration or by the uncoupling of oxidative phosphorylation. The biological activity involves inhibition of DNA synthesis [32] by creating lesions in DNA strands by oxidative rupture and by binding the nitrogen bases or DNA or RNA, hindering or blocking base replication. The inhibition growth may be due to the effect on the biosynthesis of phospholipids in cell membrane and proteins.

Among the studied compounds, $[CuL^1(OAc)]$ complex presented good activity against *C. albicans*. Since this fungi is very harmful to humans we consider this result of major importance. This confirms that antibacterial and antifungal activities are dependent on the molecular structure of the ligands and the type of the complex formed. It appears from the above results that Cu(II) Schiff base complex may be able to maintain a good antibacterial and antifungal activities and be an effective antibacterial broad-spectrum drug that may be able to solve some problem of antibacterial resistance.

In the present study, the observed cyclic voltammetric behaviour of copper complexes showed redox cycle may also contribute to their inherent toxicity. For example, redox cycling between Cu(II) and Cu(I) can catalyze the production of highly reactive hydroxyl radicals, which can subsequently damage lipids, proteins, DNA and other biomolecules. Further, the potential reduction of the Cu(II)/Cu(I) process is related to the potential SOD mimetic activity. The synthesized copper complexes also have reduction potential greater than −0.6 V, it is possible for electron uptake to occur in the biologic milieu, followed by donation to an acceptor.

The antibacterial activity of the title compounds distinctly depends on the nature of pharmacophoric moieties and their location in the 3-hydroxyflavone.

- Incorporation of thiosemicarbazide moiety in complex L^5 demonstrated higher antimicrobial activity than other complexes.
- Introduction of 4-aminoantipyrine moiety in the 3-hydroxyflavone derivatives, complex L^1 showed higher antimicrobial activity than those complexes L^2–L^4.
- Introduction of thiazole group in the 3-hydroxyflavone derivatives, the complex L^3 showed higher antimicrobial activity than that of complexes of L^1 and L^4.
- Introduction of carboxylic acid moiety in the 3-hydroxyflavone derivatives, the complex L^4 showed higher antimicrobial activity than that of complexes of L^2.

The increasing order of antimicrobial activity for the designed targeted complexes as shown below:

$[CuL^5(H2O)] > [CuL^4(OAc)] > [Cu(L^1)(OAc)] > [CuL^3(H2O)] > [CuL^2(H2O)]$

5.6. DNA binding studies

DNA binding studies are important for the rational design and construction of new and more efficient drugs targeted to DNA [33–35]. A variety of small molecules interact reversibly with double-stranded DNA, primarily through three modes: (i) electrostatic interactions with the negative charged nucleic sugar–phosphate structure, which are along the external DNA double helix and do not possess selectivity; (ii) binding interactions with two grooves of DNA double helix; and (iii) intercalation between the stacked base pairs of native DNA. In order to explore the mode of the Cu(II) complex binding to DNA, the following experiments have been carried out.

5.7. Electronic absorption study

The absorption spectra of the $[CuL^1(OAc)]$ complex in the absence and presence of DNA is shown in Supplementary figure. In

the UV region, the Cu(II) complex exhibits two absorption bands: one at ca. 354 nm and another at ca. 297 nm. With increasing DNA concentration, the absorption bands of the complexes were affected, resulting in a hypochromism tendency and slight shifts to longer wavelengths, which indicates that the Cu(II) complex can interact with DNA. The observed hypochromism and bathochromism for the Cu(II) complex are large compared to those observed for potential intercalators. The intrinsic binding constant (K_b) was obtained by monitoring the change in absorbance with increasing concentrations of DNA for the Cu(II) complexes (Table 6).As a result, binding constants of the copper complexes to DNA follow the order from high to low:

$[CuL^5(H_2O)] > [CuL^4(OAc)] > [Cu(L^1)(OAc)] > [CuL^3(H_2O)] > [CuL^2(H_2O)]$

5.8. Viscosity measurements

To further confirm the interaction mode of the Cu(II) complex with DNA, a viscosity study was carried out. The viscosity measurement is based on the flow rate of a DNA solution through a capillary viscometer. The specific viscosity contribution (g) due to the DNA in the presence of a binding agent was obtained. A classical intercalation model usually resulted in lengthening the DNA helix, as base pairs were separated to accommodate the binding ligand leading to the increase of DNA viscosity. As seen in Fig. 2 the viscosity of CT DNA increases as increase in the ratio of complexes to CT DNA. The result further suggested an intercalative binding mode of the complexes with CT DNA and also parallelled to the above spectroscopic results, such as hypochromism, blue-shift of complexes in the presence of DNA. The viscosity studies provide a strong evidence for intercalation. The viscosity increase of DNA is ascribed to the intercalative binding mode of the drug because this could cause the effective length of the DNA to increase [36].

5.9. Chemical nuclease activity

Chemical nuclease activity of copper complexes were studied using gel electrophoresis It is known that chemical nuclease activity is controlled by relaxation of supercoiled circular conformation of pUC19DNA to nicked circular and/or linear conformation. The DNA cleavage of ligand alone is inactive in the presence and absence of any external agents (data not shown). The results indicate the importance of the copper in the complex for observing the chemical nuclease activity.

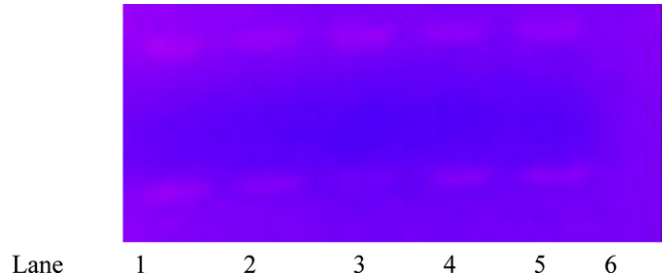

Fig. 3. Agarose gel electrophoresis of copper complexes lane 1: DNA alone; lane 2: DNA + $[CuL^1(OAc)H_2O]$ complex + H_2O_2 lane 3: DNA + $[CuL^2(H_2O)]$ complex + H_2O_2; lane 4: DNA + $[CuL^3(H_2O)]$ complex + H_2O_2; lane 5: DNA + $[CuL^4(H_2O)]$ complex + H_2O_2; lane 6: DNA + $[CuL^5(H_2O)]$ complex + H_2O_2.

The cleavage of pUC19DNA (Fig. 3) in the presence of H_2O_2 (5 mM) has been studied by gel electrophoresis using supercoiled (SC) pUC19DNA (0.2 μg, 33.3 μM) in 50mMTris–HCl/50 mM NaCl buffer (14 μL, pH 7.2) and the complexes (50 μM). In the present study, the pUC19DNA gel electrophoresis experiment was conducted at 35 °C using our synthesized complexes in the presence of H_2O_2 as an oxidant. As can be seen from the results in Fig. 3, copper complexes exhibit nuclease activity in the presence of H_2O_2. Control experiment using DNA alone (lane 1) does not show any significant cleavage of pUC19DNA even on longer exposure time. From the observed results, we conclude that the copper complexes (lane 2 and 6) were completely degraded as compared to control DNA. This shows that a slight increase in concentration over the optimal value (*i.e.*, the value at which 100% cleavage efficiency was observed) led to extensive degradations, resulting in disappearance of bands on agarose gel (Lane 6). As a result, the DNA cleavage abilities of copper complexes in the following order:

$[CuL^5(H2O)] > [CuL^4(OAc)] > [Cu(L^1)(OAc)] > [CuL^3(H_2O)] > [CuL^2(H_2O)]$

It is evident that the complexes cleave DNA more effectively in the presence of an oxidant (except lane 2), which may be due to the reaction of hydroxyl radical with DNA. These hydroxyl free radicals participate in the oxidation of the deoxyribose moiety, followed by hydrolytic cleavage of the sugar phosphate backbone [37].

In order to confirm the result obtained from 2-deoxy-D-ribose degradation & Rhodamine B dye degradation methods and to compare the ability of the copper complexes to generate hydroxyl radicals under physiological conditions. Quantification by 2-deoxy-D-ribose under the conditions of 2-mercaptoethanol and H_2O_2

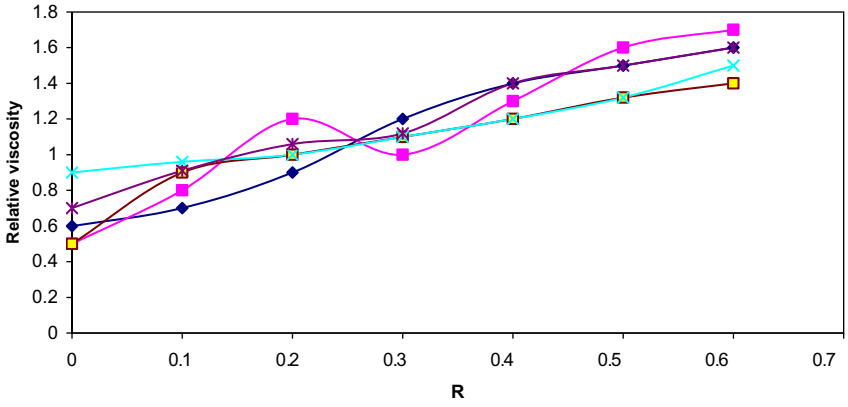

Fig. 2. Plot of relative viscosity versus [complex]/[DNA] effect of copper complex on the viscosity of CT DNA at 25 ± 0.1 °C. Copper complex = 0 – 100 μM [DNA] = 50 μM.

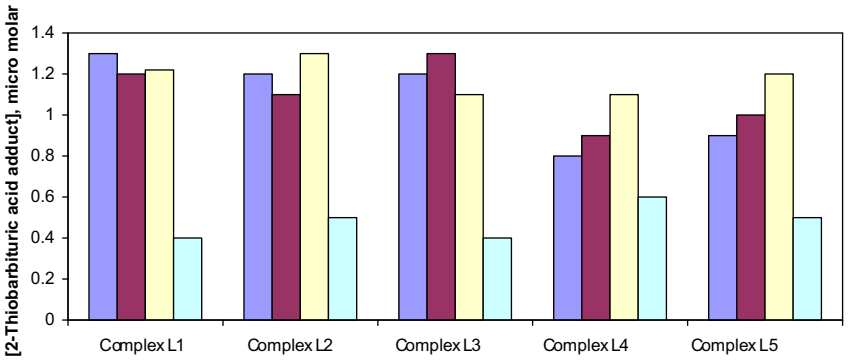

Fig. 4. Assay of hydroxyl radical production of 2-deoxy-D-ribose (400 μM) by formation 2-thiobarbiturate with copper complexes (100 μM) in 1 mm phosphate buffer. Reaction conditions: 1. activation by 50 mM 2-mercaptoethanol and 50 mM H_2O_2, simultaneous addition with each copper complex; 2. activation by 50 mM 2-mercaptoethanol and 50 mM H_2O_2, simultaneous addition with each copper complex; 3. activation by 50 mM 2-mercaptoethanol and 50 mM H_2O_2, after each copper complex has been reacted with DNA for 30 min and 4. quenching of activation reaction of 50 mM 2-mercaptoethanol and 50 mM H_2O_2 by 250 mM mannitol.

activations is shown in Fig. 4. It demonstrated that the production power of the hydroxyl radical decrease in the following order:

$[CuL^5(H2O)] > [CuL^4(OAc)] > [Cu(L^1)(OAc)] > [CuL^3(H_2O)] > [CuL^2(H_2O)]$

The degradation of the Rhodamine B dye (552 nm) provides a direct measure of the concentrations of hydroxyl radicals in the reaction mixture (Fig. 5). From the observed results, it suggested that the reactive oxygen species (hydroxyl radical) can be produced by the copper complex in the presence of oxidant.

The SOD mimetic activity values (IC_{50}) of synthesized complexes are given in Table 6. In a variety of complexes which act as Superoxide dismutase enzymes [37], there is either one-electron oxidation followed by reduction of a metal ion or formation of a Superoxide complex which then is reduced to peroxide by another Superoxide ion. In order to explore the mechanism, absorption spectrum of complexes were recorded in the presence and absence of alkaline DMSO (alkaline DMSO acts as a source of O^{2-}). The spectrum peaks became suppressed in alkaline DMSO containing buffer (pH 8.6). However upon addition of NBT, which acts as O^{2-} scavenger, these peaks were reverted to their original position. Thus, this experiment indicates that O^{2-} is initially attached to the metal complexes which later are reduced by another O^{2-} ion. The results report the scavenging ability of each complex, giving its final concentration that produced efficient quenching of the superoxide anion radical.

In the present study, the higher SOD mimetic activity of copper complexes than that of native enzyme is due to the presence of easily labile acetate ion and also azomethine containing stabilize the the Cu(I) complex formed during superoxide dismutation reaction which further reacts with superoxide ion to give hydrogen peroxide. The distorted geometry of these complexes may favour the geometrical change, which is essential for the catalysis as the geometry of copper in the SOD enzyme also changes from distorted square planar geometry. The difference in reactivities of the synthesized complexes may be attributed to the coordination environment and the redox potential of the couple Cu^{+}/Cu^{++} in copper(II) complexes during the catalytic cycle. The above results also supported from the "f" factor obtained from ESR spectra.

Antioxidants are defined as substances that even at low concentration significantly delay or prevent oxidation of easy oxidizable substrates. There is an increased interest of using antioxidants for medical purposes in the recent years. Thus, drugs possessing antioxidant and free radical scavenging properties are considered for preventing and/or treatment of diseases, which are directly related to the lack of the antioxidant capacity of the organisms. Many non-steroidal anti-inflammatory drugs have been reported to act either as inhibitors of free radical production or as radical scavengers [38]. It is well known that free radicals play an important role in inflammatory action [39]. Consequently, compounds with antioxidant properties could be expected to offer protection in inflammation and lead to potentially effective drugs. In fact, many non-steroidal anti-inflammatory drugs have been

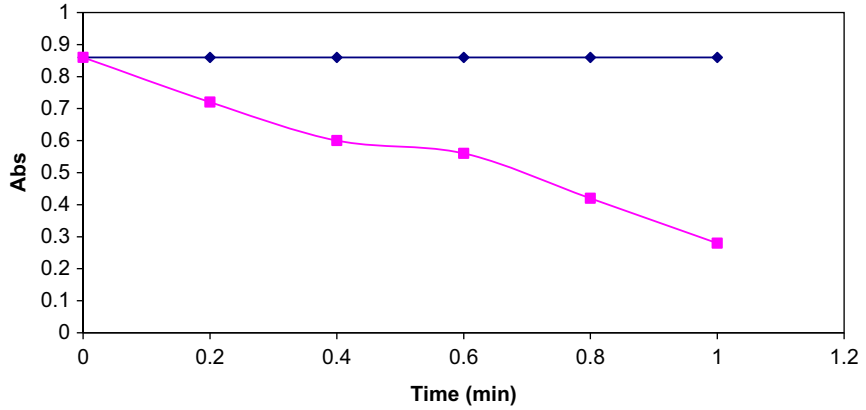

Fig. 5. Rhodamine B degradation followed by decrease of absorbance at 552 nm, pH 8.1 in10 mM phosphate buffer: (a) In presence of 0.1 mM copper complex and (b) In presence of 0.1 mM copper complex, 1 mM H_2O_2 and 10 mM ascorbic acid.

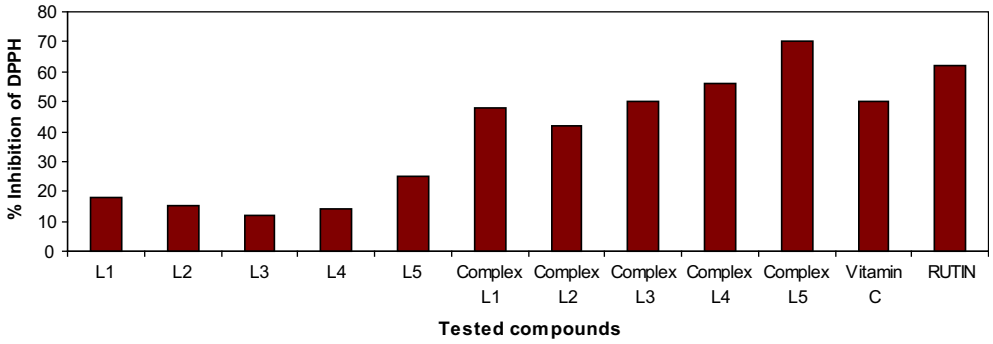

Fig. 6. Inhibition of DPPH by ligands and complexes, with rutin and C vitamin as control. All compounds were at 10 μM.

reported to act either as radical scavengers or as inhibitors of free radical production.

The DPPH method is described as a simple, rapid and convenient method independent of sample polarity for screening many samples for radical scavenging activity [39]. The antioxidant activity of complexes is presented in Fig. 6. At 10 μM concentration, complex L^4 showed a much stronger DPPH scavenging activity (58.2%) than other ligands and their complexes. The positive controls, rutin and vitamin C showed 58% and 46% DPPH scavenging, respectively. The marked antioxidant activity of complex L^4, in comparison to free ligands and other complexes, could be due to the coordination of copper in the 4 and 5 positions of the condensed ring system (A and C ring), increasing its capacity to stabilize unpaired electrons and, thereby, to scavenge free radicals. In addition, incorporation of thiazole moiety in the hydroxyflavone derivatives further enhanced the antioxidant activity. Complex of L^1 showed higher antioxidant activity than vitamin C is due to the introduction of p-substituted ($-OCH_3$) phenyl moiety in the hydroxyflavone derivatives. It implied that copper complex of L^4 might be considered as new promising lead candidates for further design and synthesis of antioxidants.

5.10. Anti-tuberculosis activity

It is seen from the results of antimycobacterial activity (Table 8), complexes were found to be highly active with MIC values, which is well below the MIC values of standard drugs. Complex of L^4 was found to be a more active antimycobacterial agent than ethambutol (due to the presence of SH group at ortho position).

5.11. Catalytic activity

The catalytic conversion of benzene to phenol was performed in acetonitrile under argon atmosphere in the presence of hydrogen peroxide as the oxidant, copper complexes act as catalysts and *o*-dichlorobenzene as internal standard for quantitative

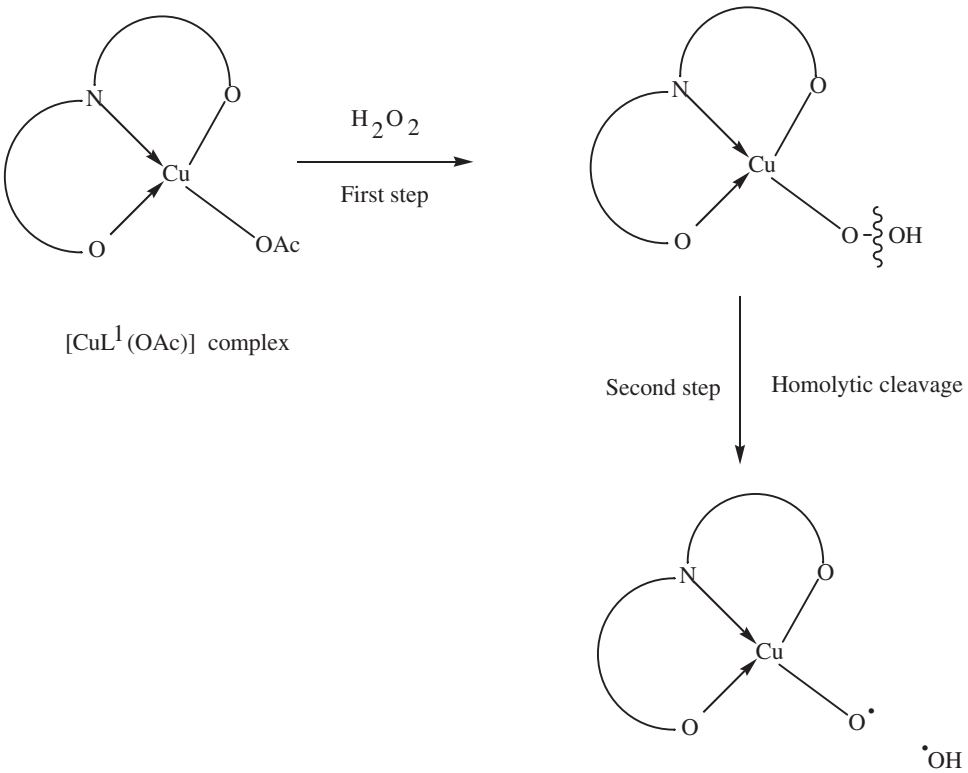

Scheme 3. Proposed reaction mechanism for catalytic conversion.

analysis by gas chromatography. Solvent, catalyst (1 mM), substrate (1 M), a small amount of oxidant and *o*-dichlorobenzene (2 M) were added successively. The total volume of reaction was 2 ml and it was allowed to stir at 25 °C for 20 h the reaction was quenched by the addition of excess of triphenylphosphine and hexane. The reaction mixture was filtered with a silica bed. The products were analyzed by gas chromatography. The proposed reaction mechanism was shown in Scheme 3. In the case of copper complex L^1, first step, copper–hydroperoxo intermediate species is formed by the reaction of copper complex L^1 with hydrogen peroxide. Second step, copper–hydroperoxo species undergoes haemolytic cleavage of the O–O bond to generate hydroxyl radical which reacts with benzene to form phenol. The turnover number for this reaction is 6.2.

6. Conclusion

The new Schiff base ligands and their copper complexes have been synthesized and characterized. The DNA binding properties of copper complexes were studied by using absorption spectra, viscosity and thermal denaturation experiments. The results show that the complexes were interacting with CT DNA. We also carried out the DNA cleavage by using gel electrophoresis techniques. From the antimicrobial study, the presence of lipophilic and polar substituent's such as C=N, S–H and NH_2 are expected to enhance the fungal and bacterial toxicity and therefore copper(II) complexes have a greater chance of interaction with the nucleotide bases. It also has been observed that some moieties such as azomethine linkage or heteroaromatic nucleus introduced into such compounds exhibit extensive biological activities that may be responsible for the increase in hydrophobic character and liposolubility of the molecules in crossing the cell membrane of the microorganism and enhance biological utilization ratio and activity of complexes. The present work has thus shown that copper complexes of Schiff base derivatives of 4-aminoantipyrine yield highly potent SOD mimics. The observed correlation between the SOD activity and the redox potential of the Cu^+/Cu^{2+} emphasizes the roles played by the electronic as well as stereo chemical factors in the biological activities of these complexes. Further work to investigate this role of copper ions by determining the lethal dose of the complex in biological systems and their pharmacological screening is in progress and will be reported in due course.

7. Experimental

The chemicals used were of AnalaR grade. Copper(II) acetate was obtained from Merck. Micro analytical data and FAB Mass spectra of the compounds were recorded at the Regional Sophisticated Instrumentation Center, Central Drug Research Institute (RSIC, CDRI), Lucknow. The amount of copper present in the copper complexes was estimated using ammonium oxalate method. The NMR spectra of the ligands were recorded using TMS as internal standard (Model: Mercury Plus 300 MHz NMR SPECTROMETER). Chemical shifts (δ) are expressed in units of parts per million relative to TMS. The FAB mass spectrum of the ligands and their complexes were recorded on a JEOL SX 102/DA-6000 mass spectrometer/data system using argon/xenon (6 kV, 10 mA) as the FAB gas. The accelerating voltage was 10 kV and the spectra were recorded at room temperature using *m*-nitrobenzylalcohol (NBA) as the matrix. Molar conductance of the copper complexes was measured in DMSO solution using a coronation digital conductivity meter. The IR spectra of the ligands and their copper complexes were recorded on a Perkin–Elmer 783 spectrophotometer in 4000–200 cm^{-1} range using KBr disc. Electronic spectra were recorded with a Systronics 2201 Double beam UV–Vis., spectrophotometer in the 200–1100 nm region. The magnetic susceptibility values were calculated using the relation $\mu_{eff} = 2.83$ (χ_mT). The diamagnetic corrections were made by Pascal's constant and Hg $[Co(SCN)_4]$was used as a calibrant. The ESR spectra of the copper complexes were recorded at 300 and 77 K on a Varian E112 X-band spectrometer. Cyclic voltammetric measurements were performed using a glassy carbon working electrode, Pt wire auxiliary electrode and an Ag/AgCl reference electrode. Tetrabutylammoniumperchlorate (TBAP) was used as the supporting electrolyte. All solutions were purged with N_2 for 30 min prior to each set of experiments. The X-ray diffractometer system JEOL JDX 8030 was used to record powder data for the copper complexes, at Central Electrochemical Research Institute, Karaikudi. Solutions of CT DNA in 50 mM NaCl/5 mM Tris–HCl (pH = 7.0) gave a ratio of UV absorbance at 260 and 280 nm, A_{260}/A_{280} of *ca*. 1.8–1.9, indicating that the DNA was sufficiently free of protein contamination. The DNA concentration was determined by the UV absorbance at 260 nm after 1:100 dilutions. The molar absorption coefficient was taken as 6600 M^{-1} cm^{-1}. Stock solutions were kept at 4 °C and used after not more than 4 days.

7.1. Preparation of ligand (L^1–L^5)

Equimolar amount of 3-hydroxyflavone and 4-aminoantipyrine (L^1)/*o*-aminophenol (L^2)/*o*-aminobenzoic acid (L^3)/*o*-aminothiazole (L^4)/thiosemicarbazide (L^5) were dissolved in ethanol (40 mL). Acetic acid (1.0 mL) was added to this solution. The solution was stirred for 3 h and precipitates formed. The precipitate was filtered and washed with water and ethanol.

L^1: Yield: 78%. Anal. Calcd for $C_{26}H_{21}N_3O_3$: C, 73.74; H, 4.99; N, 9.90. Found: C, 73.67; H, 4.91; N, 9.84. FAB mass spectrometry (FAB-MS): *m*/*z* 424 [M+1]. ^{1}H NMR (300 MHz, $CDCl_3$, δ, ppm) : 6.6–7.5 (14H, m, Ar–H), 1.6 (3H, s, H_3C–C), 1.9 (s, 3H, H_3C–N) and 10.8 (1H, s, O–H, D_2O exchangeable). ^{13}C NMR (300 MHz, $CDCl_3$, ppm): 12.5 (H_3**C**–C), 19.6 (H_3**C**–N), 143.5 (H_3C–**C**), 162.8 (**C**=O), 154.5 (=C–N), 124.6 (C-2), 118.8 (C-3), 152.6 (C-4), 119.2 (C-5), 146.4 (C-6), 125.2 (C-7), 126.4 (C-8), 157.3 (C-9), 121.6 (C-10), 133.8 (C-1′), 127.4 (C-2′, 6′), 141.8 (C-3′, 5′), 133.5 (C-4′), 127.2 (C-1″), 119.6 (C-2″, 6″), 118.9 (C-3″, 5″) and 121.6 (C-4″).

L^2: Yield: 62%. Anal. Calcd for $C_{21}H_{15}NO_3$: C, 76.58; H, 4.59; N, 4.25. Found: C, 76.52; H, 4.56; N, 4.20. FAB mass spectrometry (FAB-MS), *m*/*z* 330 [M+1]. ^{1}H NMR (300 MHz, $CDCl_3$) δ: 6.4–7.6 (13H, m, Ar–H) and 11.5 and 10.6 (2H, s, O–H, D_2O exchangeable, 3-hydroxyflavone and o-aminophenol moities). ^{13}C NMR (300 MHz, $CDCl_3$, ppm): 151.6 (C-2), 103.8 (C-3), 155.2 (C-4), 143.5 (C-5), 145.8 (C-6), 122.6 (C-7), 125.3 (C-8), 153.5 (C-9), 119.4 (C-10), 131.5 (C-1′), 123.8 (C-2′, 6′), 125.6 (C-3′, 5′), 127.2 (C-4′), 132.6 (C-1″), 116.4 (C-2″), 121.8 (C-3″), 120.6 (C-4″), 127.4 (C-5″) and 141.6 (C-6″).

L^3: Yield: 66%. Anal. Calcd for $C_{22}H_{15}NO_4$: C, 73.94; H, 4.23; N, 3.91. Found: C, 73.89; H, 4.18; N, 3.90. FAB mass spectrometry (FAB-MS), *m*/*z* 358 [M+1]. ^{1}H NMR (300 MHz, $CDCl_3$) δ : 6.8–7.6 (13H, m, Ar–H), 11.4 and 10.8 (2H, s, O–H, D_2O exchangeable, 5-hydroxyflavone and o-aminobenzoic acid moities). ^{13}C NMR (300 MHz, $CDCl_3$, ppm): 148.2 (C-2), 111.5 (C-3), 155.4 (C=N), 116.2 (C-5), 147.1 (C-6), 123.5 (C-7), 127.2 (C-8),153.4 (C-9), 120.6 (C-10), 133.6 (C-1′), 126.3 (C-2′, 6′), 128.6 (C-3′, 5′), 127.2 (C-4′), 149.1 (C-1″), 114.0 (C-2″), 132.6 (C-3″), 117.5 (C-4″), 129.4 (C-5″), 141.8 (C-6″) and 167.5 (COOH).

L^4: Yield: 68%. Anal. Calcd for $C_{21}H_{15}NO_2S$: C, 67.49; H, 3.78; N, 8.75. Found: C, 67.42; H, 3.72; N, 8.69. Fast atom bombardment mass spectrometry (FAB-MS), *m*/*z* 322 [M+1]. ^{1}H NMR (300 MHz, $CDCl_3$) δ: 5.1 & 5.4 (2H, dd, *J*, 10.5 Hz,–CH = CH-), 5.9–7.9 (9H, m, Ar–H), 12.9 (1H, s, O–H, D_2O exchangeable). ^{13}C NMR (300 MHz, $CDCl_3$) : 148.5 (C-2), 111.4 (C-3), 155.6 (C=N), 116.8 (C-5), 148.2 (C-

6), 123.6 (C-7), 127.8 (C-8), 155.5 (C-9), 122.4 (C-10), 133.6 (C-1′), 126.2 (C-2′, 6′), 128.4 (C-3′, 5′), 127.6 (C-4′), 159.4 (C-11), 104.6 (C-12) and 149.5 (C-13).

L^5: Yield: 70%. Anal. Calcd for $C_{16}H_{13}N_3O_2S$: C, 61.72; H, 4.20; N, 13.49. Found: C, 61.65; H, 4.15; N, 13.40. Fast atom bombardment mass spectrometry (FAB-MS), *m/z* 311 [M+1]. ^{1}H NMR (300 MHz, $CDCl_3$) δ: 6.8–7.6 (8H, m, Ar-H), 11.2 (1H, s, –NH), 8.3 (1H, s, br, HN of $-NH_2$), 7.6 (1H, s, br, HN of $-NH_2$), 11.9 (1H, s, O–H, D_2O exchangeable). ^{13}C NMR (300 MHz, $CDCl_3$): 167.7 (C═O), 150.6 (C-2), 112.5 (C-3), 155.8 (C═N), 116.8 (C-5), 147.4 (C-6), 124.6 (C-7), 125.6 (C-8), 153.4 (C-9), 119.5 (C-10), 133.5 (C-1′), 126.0 (C-2′, 6′), 126.8 (C-3′, 5′), 127.9 (C-4′) and 176.2 (C═S).

7.2. Preparation of copper complexes of ligands (L^1–L^5)

The ligand (*s*) (0.05 mM) and copper acetate (0.05 mM) were dissolved in acetone (20 mL). Under stirring, triethylamine (0.075 mM) was then dropped to the mixture with caution. After stirring for 4 h at room temperature, the precipitate was separated by suction filtration, purified by washing several times with acetone and dried in vaccum.

Complex of L^1: Yield: 68%. Anal. Calcd for $CuC_{28}H_{24}N_3O_5$: C, 61.57; H, 4.43; N, 7.70, Cu, 11.64. Found: C, 61.50; H, 4.39; N, 7.68; Cu, 11.65. FAB mass spectrometry (FAB-MS), *m/z* 545 [M+1]. μ_{eff} (BM) = 1.96; Λ_m (mhocm^2 mol^{-1}) = 20.

Complex of L^2: Yield: 76%. Anal. Calcd for $CuC_{21}H_{17}NO_4$: C, 61.36; H, 4.17; N, 3.41, Cu, 15.47. Found: C, 61.31; H, 4.15; N, 3.36; Cu, 15.43. FAB mass spectrometry (FAB-MS), *m/z* 411 [M+1]. μ_{eff} (BM) = 1.94; Λ_m (mhocm^2 mol^{-1}) = 22.

Complex of L^3: Yield: 69%. Anal. Calcd for $CuC_{22}H_{17}NO_5$: C, 60.18; H, 3.91; N, 3.19, Cu, 14.49. Found: C, 60.14; H, 3.86; N, 3.15; Cu, 14.43. FAB mass spectrometry (FAB-MS), *m/z* [M+1]. μ_{eff} (BM) = 2.04; Λ_m (mhocm^2 mol^{-1}) = 16.

Complex of L^4: Yield: 76%. Anal. Calcd for $CuC_{21}H_{17}NO_3S$: C, 54.22; H, 3.42; N, 6.33; Cu, 14.36. Found: C, 74.62; H, 3.35; N, 6.29; Cu, 14.31. FAB mass spectrometry (FAB-MS), *m/z* 443 [M+1]. μ_{eff} (BM) = 1.98; Λ_m (mhocm^2 mol^{-1}) = 18.

Complex of L^5: Yield: 60%. Anal. Calcd for $CuC_{16}H_{14}N_3O_3S$: C, 48.90; H, 3.85; N, 10.70; Cu, 16.18. Found: C, 74.62; H, 3.81; N, 10.63; Cu, 16.14. FAB mass spectrometry (FAB-MS), *m/z* 393[M+1]. μ_{eff} (BM) = 2.06; Λ_m (mhocm^2 mol^{-1}) = 20.

7.3. Antimicrobial activity

The *in vitro* antimicrobial activities of the investigated compounds were tested against the bacterial species and fungal species. One day prior to the experiment, the bacterial and fungal cultures were inoculated in broth (inoculation medium) and incubated overnight at 37 °C. Inoculation medium containing 24 h grown culture was added aseptically to the nutrient medium and mixed thoroughly to get the uniform distribution. This solution was poured (25 mL in each dish) into petri dishes and then allowed to attain room temperature. Wells (6 mm in diameter) were cut in the agar plates using proper sterile tubes. Then, wells were filled up to the surface of agar with 0.1 mL of the test compounds dissolved in DMSO (200 μM/mL). The plates were allowed to stand for an hour in order to facilitate the diffusion of the drug solution. Then the plates were incubated at 37 °C for 24 h for bacteria and 48 h for fungi and the diameter of the inhibition zones were read. Minimum inhibitory concentrations (MICs) were determined by using serial dilution method. The lowest concentration (μg/mL) of compound, which inhibits the growth of bacteria after 24 h incubation at 37 °C, and of fungi after 48 h incubation at 37 °C was taken as the MIC. The concentration of DMSO in the medium did not affect the growth of any of the microorganisms tested.

7.3.1. SOD activity

In vitro SOD activity was measured using alkaline DMSO as a source of superoxide radical (O_2^-) and nitrobluetetrazolium (NBT) as O_2^- scavenger [40,41]. In general, 400 μL sample to be assayed was added to a solution containing 2.1 mL of 0.2 M potassium phosphate buffer (pH 8.6) and 1 mL of 56 μM NBT. The tubes were kept in ice for 15 min and then 1.5 mL of alkaline DMSO solution was added while stirring. The absorbance was then monitored at 540 nm against a sample prepared under similar condition except NaOH was absent in DMSO. A unit of superoxide dismutase [SOD] activity is the concentration of complex or enzyme, which causes 50% inhibition of alkaline dimethylsulphoxide (DMSO) mediated reduction of nitrobluetetrazolium chloride (NBT).

7.4. Absorption titration experiment

Absorption titration experiment was performed by maintaining a constant concentration of the complex while varying the nucleic acid concentration. This was achieved by dissolving an appropriate amount of the copper complex stock solution and by mixing various amounts of DNA stock solutions while maintaining the total volume constant. This resulted in a series of solutions with varying concentrations of DNA but with a constant concentration of the complex. The absorbance (*A*) of the most red-shifted band of complex was recorded after each successive additions of CT DNA. The intrinsic binding constant, K_b, was determined from the plot of [DNA]/($\varepsilon_a-\varepsilon_f$) *vs* [DNA], where [DNA] is the concentration of DNA in base pairs, ε_a, the apparent extinction coefficient which is obtained by calculating A_{obs}/[complex] and ε_f corresponds to the extinction coefficient of the complex in its free form. The data were fitted to the following equation where ε_b refers to the extinction coefficient of the complex in the fully bound form.

$$[DNA]/(\varepsilon_a-\varepsilon_f) = [DNA]/(\varepsilon_b-\varepsilon_f) + 1/Kb(\varepsilon_b-\varepsilon_f) \quad (6)$$

Each set of data, when fitted to the above equation, gave a straight line with a slope of $1/(\varepsilon_b-\varepsilon_f)$ and a *y*-intercept of $1/K_b(\varepsilon_b-\varepsilon_f)$. K_b was determined from the ratio of the slope to intercept.

Fixed amounts of complexes were dissolved in DMSO because the high solubility of the compounds in this solvent allows us to prepare concentrated solutions and to utilize reduced volumes (5 μL) for titrations. It was also verified that the DMSO percentage (0.7%) added to the DNA solution did not interfere with the nucleic acid; in fact, the 260 nm absorption band is not subjected to modifications in intensity and position.

7.5. Viscosity measurements

Viscosity experiments were carried on an Ostwald viscometer, immersed in a thermostated water-bath maintained at a constant temperature at 30 ± 0.1 °C. Viscosity measurements were carried out at room temperature. DNA samples of approximately 0.5 mM were prepared by sonicating in order to minimize complexities arising from DNA flexibility. Flow time was measured with a digital stopwatch three times for each sample and an average flow time was calculated. Each experiment was performed three times and an average flow time was calculated. Data were represented as (η/η_0) versus binding ratio, where η is the viscosity of DNA in the presence of complex and η is the viscosity of DNA alone. Viscosity values

were calculated after correcting the flow time of buffer alone (t_0), $\eta = (t - t_0)/t_0$.

7.6. Antioxidant assay

The samples were tested individually at a final concentration of 10 μM. The solution contained 1 ml of DPPH (diphenylpicrylhydrazyl radical, 60 μM) and different concentrations of the antioxidant solutions of ligands and their complexes, resulting in a final concentration of DPPH of 30 μM. The mixtures were vigorously mixed and allowed to stand in the dark for 30 min at 25 °C. The absorbance of the resulting solutions were measured at 517 nm against a blank sample containing only DPPH, the negative control; Rutin and Vitamin C served as the positive control.

7.7. Assay of DNA cleavage

For DNA cleavage study, buffer solutions of 50 μ*mol* Tris–HCl/18 mmol NaCl in distilled water (pH 7.1) and Tris–acetic acid–EDTA in distilled water (pH 8.3) were used. The extent of cleavage of supercoiled pUC19DNA (33.3 μM, 0.2 μg) to its nicked circular form was determined by agarose gel electrophoresis in the presence of H_2O_2. The gel electrophoresis experiments were performed by incubation at 35 °C for 1.5 h as follows: pUC19DNA 10 μM, 5 μM each complex, 1 μM H_2O_2 in 50 μM tris–HCl buffer (pH = 7.2) and 30 mL of double distilled water. The samples were electrophoresed for 2 h at 50 V on 1% agarose gel using tris–acetic acid–EDTA buffer (pH = 8.3). After electrophoresis, the gel was stained using 1 μg/cm^3 ethidium bromide and photographed under UV light.

7.8. Anti-tubercular activity

In vitro evaluation of the anti-tubercular activity was carried out against *Mycobacterium tuberculosis* $H_{37}Rv$ by using broth dilution [42] assay method. The result of anti-tubercular activity is presented in Table 8.

Acknowledgement

We express our sincere thanks to the Chancellor, Noorul Islam Centre for Higher Education, Kumaracoil for providing research facilities. This study was funded by DST, New Delhi under INSPIRE fellowship (IF 10544) and CSIR, New Delhi (Grant No. 01(2497)/11/EMR-II).

Appendix. Supplementary material

Supplementary data related to this article can be found online at doi:10.1016/j.ejmech.2012.01.006.

References

[1] J.R. Nitschke, Acc. Chem. Res. 40 (2007) 103–107.
[2] T. Opstal, F. Verpoort, Angew. Chem. Int. Ed. 42 (2003) 2876–2884.
[3] C. Adhikary, R. Bera, B. Dutta, S. Jana, G. Bocelli, A. Cantoni, S. Chaudhuri, S. Koner, Polyhedron 27 (2008) 1556–1561.
[4] P.R. Kumar, S. Upreti, A.K. Singh, Polyhedron 27 (2008) 1610–1614.
[5] V. Patroniak, A.R. Stefankiewicz, J.-M. Lehn, M. Kubicki, Eur. J. Inorg. Chem. 10 (2005) 4168–4173.
[6] A. Balamurugan, G. Balossier, D. Laurent-Maquin, S. Pina, A.H.S. Rebelo, J. Faure, J.M.F. Ferreira, Dent. Mater. 24 (2008) 1343–1346.
[7] Z.H. Chohan, S. Kausar, Chem. Pharm. Bull. 41 (1993) 951–958.
[8] M. Kurtoglu, F. Purtas, S. Toroglu, Trans. Met. Chem. 33 (2008) 705–711.
[9] J.G. Horsfall, Principles of Fungicidal Action, Chronica Botanica Co., Waltham, 1956, p. 141.
[10] P. Arman, R.L. Wain, Ann. Appl. Biol. 46 (1958) 366–371.
[11] V.A. Kostyuk, A.I. Potapovich, E.N. Vladykovskaya, L.G. Korkina, I.B.A. Afanas'ev, Arch. Biochem. Biophys. 385 (2001) 129–135.
[12] P.K. Mascharak, Coord. Chem. Rev. 225 (2002) 201–208.
[13] P.H. Wang, J.G. Keck, E.J. Lien, et al., J. Med. Chem. 33 (1990) 608–614.
[14] J.R. Merchant, G. Martsyen, N.S. Venkatesh, Ind. J. Chem. Sect. B. 20 (1981) 493–498.
[15] P. Kapoor, M.K. Rastogi, R. Khanna, C.P. Garg, Ind. J. Chem. Sect. B. 20 (1981) 390.
[16] P.K. Radhakrishanan, P. Indrasen, C.G.R. Nair, Polyhedron 18 (1998) 67–73.
[17] C.C. Winterbourn, Biochem. J. 198 (1981) 125–129.
[18] Sandipan Sarkar, Pulak K. Dhara, M. Nethaji, Pabitra Chattopadhyay, J. Coord. Chem. 62 (2009) 817–822.
[19] W.J. Geary, Coord. Chem.Rev. 7 (1971) 81–114.
[20] K. Nakamoto, Spectroscopy and Structure of Metal Chelate Compounds, John Wiley, New York, 1988, p. 214.
[21] J.R. Anacona, Daniel Lorono, Mary azocar, Reinaldo Atencio, J. Coord. Chem. 62 (2009) 951–956.
[22] A.B.P. Lever, Inorganic Electronic Spectroscopy, second ed. Elsevier, New York, 1968.
[23] P.K. Ray, B. Kauffman, Inorg. Chim. Acta 173 (1990) 207–211.
[24] B.J. Harthway, A.A.G. Tomlinson, Coord. Chem. Rev. 5 (1970) 1–43.
[25] A.W. Addison, Inorg. Chim. Acta 162 (1989) 217–220.
[26] T.R. Li, Z.Y. Yang, B.D. Wang, D.D. Qin, Eur. J. Med. Chem. 43 (2008) 1688.
[27] C.M. Kepert, G.B. Deacon, L. Spiccia, Inorg. Chim. Acta 355C (2003) 211–220.
[28] A.S. Gaballa, M.S. Asker, A.S. Barakat, S.M. Teleb, Spectrochim. Acta A 67 (2007) 114–118.
[29] Y. Liu, Na. Wang, W. Mei, F. Chen, H. Li-Xin, L. Jian, R. Wang, Transit. Met. Chem. 32 (2007) 332–337.
[30] Alicia M. Díaz, Reynaldo Villalonga, Roberto Cao, J. Coord. Chem. 62 (2009) 100.
[31] N. Dharamaraj, P. Viswanathamurthi, K. Natarajan, Transit. Met. Chem. 26 (2001) 105–111.
[32] R.N. Patel, N. Singh, K.K. Shukla, U.K. Chauhan, J. Nicols Gutierrez, A. Castineiras, Inorg. Chim. Acta 357 (2004) 2469–2476.
[33] S. Parveen, F. Arjmand, Indian J. Chem. 44A (2005) 1151–1156.
[34] Q.S. Li, P. Yang, H.F. Wang, M.L. Guo, J. Inorg. Biochem. 64 (1996) 181–186.
[35] J. Liu, H. Zhang, C. Chen, H. Deng, T. Lu, L. Ji, J. Chem. Soc. Dalton Trans. (2003) 114–120.
[36] M.C. Prabahara, H.S. Bhojya Naik, Biometals 21 (2008) 675–684.
[37] L.A. Sandan, G. Elias, M.N.A. Gao, Arzneim.-Forsch 40 (1990) 89–93.
[38] I. Kruk, in: O. Hutzinger, I. Kruk (Eds.), The Handbook of Enviromental Chemistry. Reactions and Processes, Part 1, Springer Verlag, Berlin, 1998.
[39] W.K. Pogozelski, T.D. Tullius, Chem. Rev. 98 (1998) 1089–1096.
[40] Panchangam Murali Krishna, Katreddi Hussain Reddy, Jay Prakash Pandey, Dayananda Siddavattam, Transit. Met. Chem. 33 (2008) 661–668.
[41] S. Dhar, P.A.N. Reddy, M. Nethaji, S. Mahadevan, M.K. Saha, A.R. Chakravarty, Inorg. Chem. 41 (2002) 3469–3475.
[42] D.M. Yajko, J.J. Madej, M.V. Lacaster, C.A. Sanders, V.L. Cawthon, B. Gee, A. Babst, W. Keith Hardley, J. Clin. Microb. 33 (1995) 2324–2327.